

See discussions, stats, and author profiles for this publication at: <https://www.researchgate.net/publication/231646109>

Highly Stabilized and Finely Dispersed Cu₂O/TiO₂: A Promising Visible Sensitive Photocatalyst for Continuous Production of Hydrogen from Glycerol:Water Mixtures

ARTICLE in THE JOURNAL OF PHYSICAL CHEMISTRY C · NOVEMBER 2010

Impact Factor: 4.77 · DOI: 10.1021/jp107405u

CITATIONS

110

READS

371

6 AUTHORS, INCLUDING:



Dr. Sadanandam Gullapelli

Indian Institute of Chemical Technology

11 PUBLICATIONS 212 CITATIONS

SEE PROFILE



Machiraju Subrahmanyam

Indian Institute of Chemical Technology

39 PUBLICATIONS 920 CITATIONS

SEE PROFILE



Sreedhar Bojja

Indian Institute of Chemical Technology

464 PUBLICATIONS 7,721 CITATIONS

SEE PROFILE



Neha Hebalkar

International Advanced Research Centre fo...

44 PUBLICATIONS 867 CITATIONS

SEE PROFILE

Highly Stabilized and Finely Dispersed Cu₂O/TiO₂: A Promising Visible Sensitive Photocatalyst for Continuous Production of Hydrogen from Glycerol:Water Mixtures

Kannekanti Lalitha,[†] Gullapelli Sadanandam,[†] Valluri Durga Kumari,^{*,†} Machiraju Subrahmanyam,[†] Bojja Sreedhar,[†] and Neha Y. Hebalkar[‡]

Inorganic and Physical Chemistry Division, Indian Institute of Chemical Technology, Hyderabad-500607, India, and International Advanced Research Centre for Powder Metallurgy and New Materials, Hyderabad-500005, India

Received: August 6, 2010; Revised Manuscript Received: November 6, 2010

Cu-doped TiO₂ with varying amounts of Cu (0.2, 0.3, 0.5, 1, 2, and 5) are prepared by impregnation method and calcined at 350 and 450 °C for 5 h. These catalysts are characterized by X-ray diffraction, diffuse reflectance spectroscopy (DRS), X-ray photoelectron spectroscopy (XPS), scanning electron microscopy energy-dispersive X-ray spectroscopy (EDAX), and transmission electron microscopy (TEM). The DRS studies are clearly showing the expanded photo response of TiO₂ into the visible region on impregnation of copper ions. TEM images are depicting the fine dispersion of Cu particles on TiO₂ surface. XPS studies are showing change in the binding energy values of Ti 2p, O 1s, and Cu 2p, indicating that copper ions are in interaction with TiO₂. XPS results are also confirming that the oxidation state of copper is +2 in samples calcined at 350 °C and +1 in samples calcined at 450 °C. EDAX analysis supports the presence of copper species on the surface layers of TiO₂. Photocatalytic hydrogen production activity studies are conducted over CuO/TiO₂ and Cu₂O/TiO₂ catalysts in pure water and glycerol:water mixtures under solar irradiation. Maximum hydrogen production of 265 and 290 $\mu\text{mol h}^{-1}$ is observed over 2 wt % CuO/TiO₂ and Cu₂O/TiO₂ catalysts in pure water. A significant improvement in hydrogen production is observed in glycerol:water mixtures and maximum hydrogen production of 16,500 and 20,060 $\mu\text{mol h}^{-1}$ is obtained over 0.5 wt % CuO/TiO₂ and Cu₂O/TiO₂ catalysts in 5% glycerol aqueous solutions. No hydrogen production activity is observed on reduced catalysts under solar irradiation. Furthermore, when these catalysts are studied under UV irradiation, 2–3 fold increase in activity is observed on calcined catalysts, and the same level of activity is observed on reduced catalysts, but under these conditions the activity is limited by the dissolution of Cu ions into the solution. However, under solar irradiation a continuous and stable activity is observed over Cu₂O/TiO₂ catalyst. On the basis of the characterization and hydrogen production activity results, finely dispersed Cu in +1 oxidation state that is in interaction with TiO₂ is proposed as a promising visible sensitive photocatalyst for the continuous production of hydrogen from glycerol:water mixtures.

1. Introduction

For the past few decades, fossil fuels like coal, petroleum, and natural gas are playing a dominating role as energy resources. These energy resources are nonrenewable, limited in quantity, and causing serious impact on the environment. Therefore, the production of renewable and nonpolluting fuels by the direct conversion of solar energy into chemical energy is one of the priorities of the scientific community. The production of hydrogen has received much attention because of its potential application as a clean source of energy. Hydrogen production by steam reforming of fossil fuels emits CO₂. Photocatalytic hydrogen production from water splitting using solar energy may be seen as an alternative approach for this issue.

Photocatalytic water splitting in recent years is extended to use the organic pollutants and alcohols as sacrificial agents for hydrogen production.^{1,2} Using biomass-derived glycerol as feedstock for hydrogen production is gaining importance as it

is produced in large amounts and is rapidly becoming a waste with an additional disposal cost.

TiO₂ has been considered as one of the most promising photocatalysts for various reactions. But its band gap limits its usage in the visible light region. Usually, addition of nonmetals, metal ions, and dye sensitization methods are employed to extend the absorption edge of TiO₂ into visible region.^{3–5} Noble metal deposited TiO₂ catalysts are well studied for reforming reactions.^{6–10} Daskalaki et al. have reported hydrogen production by photoinduced glycerol reforming over Pt/TiO₂ catalyst. They studied the effect of temperature, pH, catalyst weight in solution, and glycerol concentration on the rate of the reaction.¹¹ Kondarides reported hydrogen production by photoreforming of biomass-derived components and derivatives over Pt/TiO₂ catalyst at ambient conditions.¹² Bowker et al. have compared the photocatalytic reforming of glycerol and methanol over Au- and Pd-modified TiO₂ catalyst and found that the rate of hydrogen production is more over Pd-modified catalyst.¹³ Luo et al. studied the hydrogen production over heteroatom doped titania from glycerol, sucrose, and fructose solutions and they found that Pt-loaded B- and N-codoped TiO₂ is showing maximum hydrogen production.¹⁴

* To whom correspondence should be addressed. E-mail: durgakumari@iict.res.in. Phone: +91-40-27193165. Fax: +91-40-27160921.

[†] Indian Institute of Chemical Technology.

[‡] International Advanced Research Centre for Powder Metallurgy and New Materials.

Use of noble metals like Pt, Au, and Pd is very expensive compared to transition metal ions, and the use of transition metals makes the material visible sensitive. Among the transition metal ions, Cu-loaded TiO₂ has been studied for hydrogen production under UV as well as solar light irradiation.^{15–22}

Earlier in our lab, we were worked on developing the new materials and sensitizing the UV active semiconductor into visible light by noble metal deposition for water splitting reaction.^{23–25}

In the present investigation Cu-loaded TiO₂ catalysts are evaluated for hydrogen production from water and glycerol: water mixture under solar irradiation and these results are compared with UV activity to elucidate the structure–activity correlation under solar irradiation.

2. Experimental Section

2.1. Chemicals. TiO₂ P-25 (anatase-80%, rutile-20%, surface area 50 m² g^{−1} and particle size 27 nm) from Degussa Corporation, Germany, Cu(NO₃)₂ from LOBA CHEMIE Pvt., Ltd., India, glycerol from Qualigens Fine Chemicals India, Ltd., are procured and used without any further purification.

2.2. Catalyst Preparation. Cu (0.2, 0.3, 0.5, 1, 2, and 5 wt %) was loaded on TiO₂ by impregnation method. For each Cu-modified sample required amount of TiO₂ was dispersed in Cu (NO₃)₂ solution in distilled water. Excess water was evaporated to dryness with slow heating and constant stirring. The sample was dried at 110 °C and calcined at 350 °C (catalyst CT-1) and 450 °C (catalyst CT-2) for 5 h.

2.3. Characterization. The X-ray diffraction (XRD) patterns of Cu-modified TiO₂ catalysts were recorded with Siemens D-5000 X-ray diffractometer using Cu K α radiation. The UV–vis diffuse reflectance spectra were recorded on a GBC UV–visible Cintra 10_e spectrometer, in the wavelength range 200–800 nm. The scanning electron microscopy (SEM) analysis of the catalysts was performed on Hitachi S-520 SEM unit. Elemental analysis was carried out using Link, ISIS-300, Oxford, energy-dispersive X-ray spectroscopy (EDAX) detector. A Philips Technai G2 FEI F12 transmission electron microscope operating at 80–100 kV was used to record the transmission electron microscopy (TEM) patterns. X-ray photoelectron spectra (XPS) were recorded on a KRATOS AXIS 165 equipped with Mg K α radiation.

2.4. Catalytic Activity. Photocatalytic reactions were carried out under solar light and UV (400 W Hg vapor lamp) light irradiation. The intensity of solar light was measured using a LT Lutron LX-101A digital light meter. The solar light intensity was measured for every hour between 10:00 and 15:00. The average light intensity value observed was around 1,30,000 lx during the experiments.

The reaction was performed in a 150-mL quartz reactor by taking 50 mL of distilled water containing 100 mg of catalyst. Reactions were also carried out in 5% glycerol:water mixtures. Prior to the irradiation, the reaction mixture was evacuated for 30 min and also purged with nitrogen gas for 30 min to remove the dissolved oxygen. After irradiation, the evolved gaseous products were analyzed at every 1 h by a gas chromatography (Shimadzu GC-2014) with molecular sieve 5A column using thermal conductivity detector and N₂ as a carrier gas. CO₂ was analyzed by using corbaxen-1000 column. For comparison and to identify the active sites the catalyst is also studied after reducing in 30% H₂ and balance N₂ at 350 °C for 3 h.

3. Results

3.1. XRD. On impregnation of copper over TiO₂, no characteristic peaks of Cu are observed in the calcined samples,

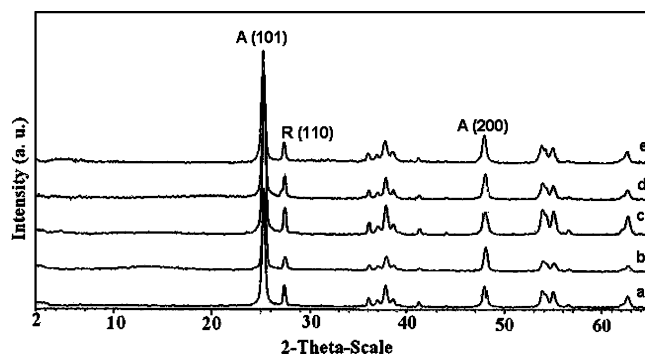


Figure 1. XRD patterns of CT-2 catalysts. Cu wt % (a) 0.2, (b) 0.5, (c) 1, (d) 2, and (e) 5.

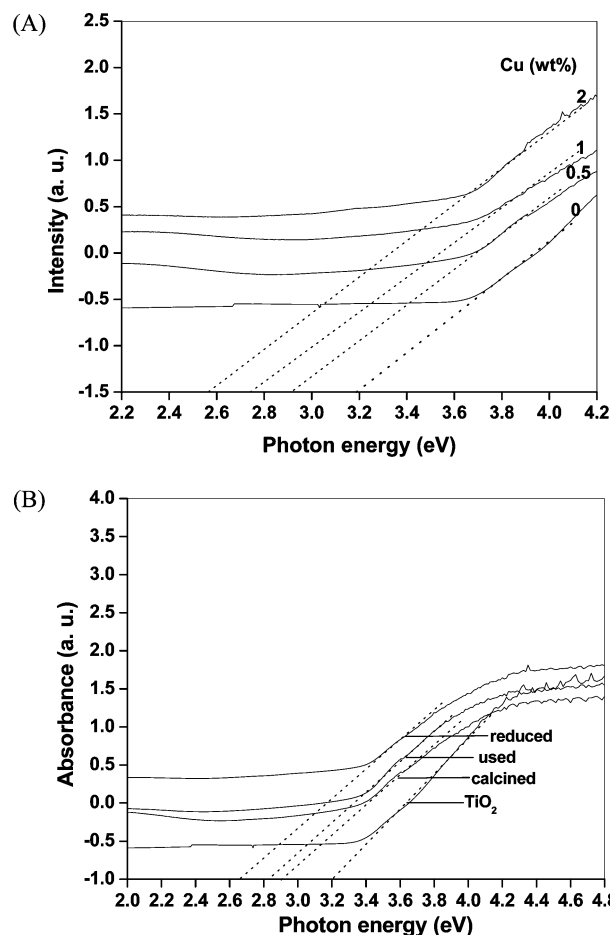


Figure 2. UV–vis DRS of (A) CT-2 catalysts with copper (wt %) loading. (B) Comparison of 0.5 wt % CT-2 calcined, used, and reduced catalysts.

and only the characteristic 101,200 planes of TiO₂ anatase and 110 of rutile are identified from the XRD results. The absence of copper peak in the calcined samples indicates the fine dispersion of copper species on the surface of TiO₂ as the copper content used in this preparation is 0.5–5 wt %. As the XRD patterns of both CT-1 and CT-2 are identical, the XRD patterns of CT-2 are shown in Figure 1 to represent both the series.

3.2. Diffuse Reflectance Spectroscopy (DRS). Figure 2A shows the diffuse reflectance spectra of TiO₂ and copper-loaded TiO₂ CT-2 catalysts. The band gap energy values are calculated from the plot of absorbance versus photon energy in electron-volts (calculated from the formula $\lambda = 1239.8/E_{\text{bg}}$). Absorbance is extrapolated to get the band gap energy, and the values for CT-1 and CT-2 catalysts are given in Table 1. TiO₂ exhibits a

TABLE 1: Physical Characteristics of Cu-Loaded TiO₂ Catalysts

catalyst (Cu (wt %)/TiO ₂)	band gap energy (eV)		Cu (wt %) by EDAX	
	CT-1	CT-2	CT-1	CT-2
0	3.2	3.2	—	—
0.2	2.93	3.13	0.17	0.18
0.3	2.86	3.05	0.29	0.285
0.5	2.81	2.91	0.49	0.48
1	2.74	2.75	0.985	0.98
2	2.52	2.56	1.89	1.92
0.5 ^a	—	2.65	—	—
0.5 ^b	2.79	2.83	0.41	0.42
0.5 ^c	2.51	2.62	0.25	0.23

^a Reduced. ^b Used under solar light. ^c Used under UV light.

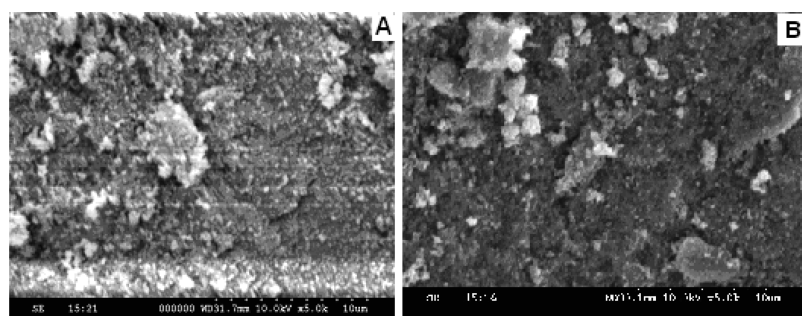
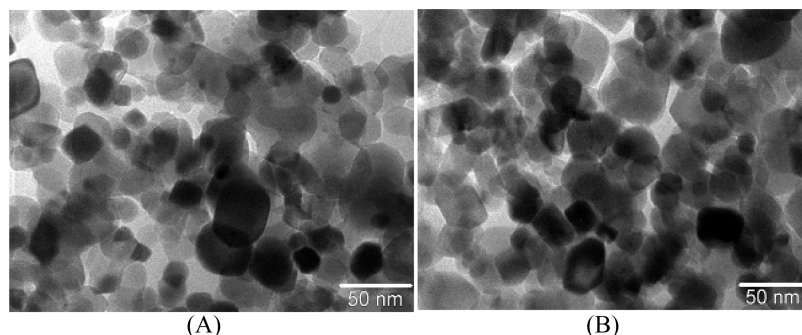
strong absorption band around 384 nm corresponding to band gap energy of 3.2 eV. On loading copper, the band edge of TiO₂ is slightly expanded into the visible region, and this may be due to the additional energy levels created by the Cu ions in the band gap of TiO₂.²⁵ With increasing copper loading over TiO₂, the band gap energy values are decreased from 3.2 eV to a minimum value of 2.56 eV on CT-2 catalysts as shown in Figure 2A. In CT-1 catalysts also the band gap values are decreased with increasing Cu loading over TiO₂ as shown in Table 1. DRS and band gap energy values of 0.5 wt % CT-2 used (under solar and UV) and thermally reduced catalysts are compared with calcined catalyst as shown in Figure 2B and Table 1. The band gap energy of the catalyst used under solar irradiation is slightly decreased (from 2.91 to 2.83 eV), and this value is much less compared to the decrease observed in the band gap of thermally reduced catalyst (2.91 to 2.65 eV) and in the catalyst used under UV irradiation (2.91 to 2.62 eV). The catalysts used under UV irradiation and thermally reduced are showing almost similar band gap (2.62 and 2.65 eV) suggesting that in these two conditions Cu₂O is reduced to the same extent as shown in Table 1. As the difference in the conduction and valence bands is less in the reduced form (Cu⁰)

compared to the oxide form, the band gaps are decreased in reduced catalysts. However under solar irradiation, even after using the catalyst for 40 h, the decrease in the band gap is very less (0.08 eV) indicating that the catalyst is stable under solar irradiation. This is also in confirmation with the XPS results of used catalyst under solar irradiation wherein Cu⁰ is not seen. However the small decrease observed in the band gap of 0.5 wt % CT-2 used catalyst under solar irradiation may be seen as due to the presence of Cu species with oxidation state < 1. From the DRS results it is clear that copper loading can shift the absorption edge of TiO₂ into the visible region, which in turn decreases the band gap for improving the photo absorption and photocatalytic performance of TiO₂ in visible region.

3.3. SEM-EDAX. The morphology of TiO₂ and CT-2 catalysts is investigated by SEM and shown in Figure 3. The surface morphology of TiO₂ seems to be changed after Cu loading and appears slightly dark. EDAX analysis of samples was carried out to determine the copper content on the surface of TiO₂, and the data obtained is shown in Table 1. The results clearly indicate the presence of copper ions on the surface of TiO₂ in the calcined catalysts. In the used catalysts loss of Cu is much less under solar irradiation (for 0.5 wt % CT-1 catalyst, 0.49 to 0.41; for 0.5 wt % CT-2 catalyst, 0.48 to 0.42), and about 50% loss is observed on CT-1 as well as CT-2 catalysts under UV irradiation. The observed loss is seen as due to the dissolution of Cu ions into the solution by the acidic conditions formed during the reaction.

3.4. TEM. The TEM photographs of 0.5 wt % CT-2 calcined and used catalysts are shown in parts A and B of Figure 4. In calcined catalysts, the TiO₂ particles with copper deposition appeared dark against the surface of TiO₂. Used catalyst is also showing the same type of morphology indicating that the catalyst is intact after several hours of reaction.

3.5. XPS. XPS studies are conducted over CT-1 and CT-2 catalysts in order to understand the chemical environment of copper ions on TiO₂. XPS spectra of Ti 2p, Cu 2p, and O1s core level profiles of different wt % Cu-loaded CT-2 catalysts

**Figure 3.** SEM images of CT-2 catalysts, Cu wt % (A) 0 and (B) 1.**Figure 4.** TEM images of 0.5 wt % CT-2 catalysts (A) calcined and (B) used.

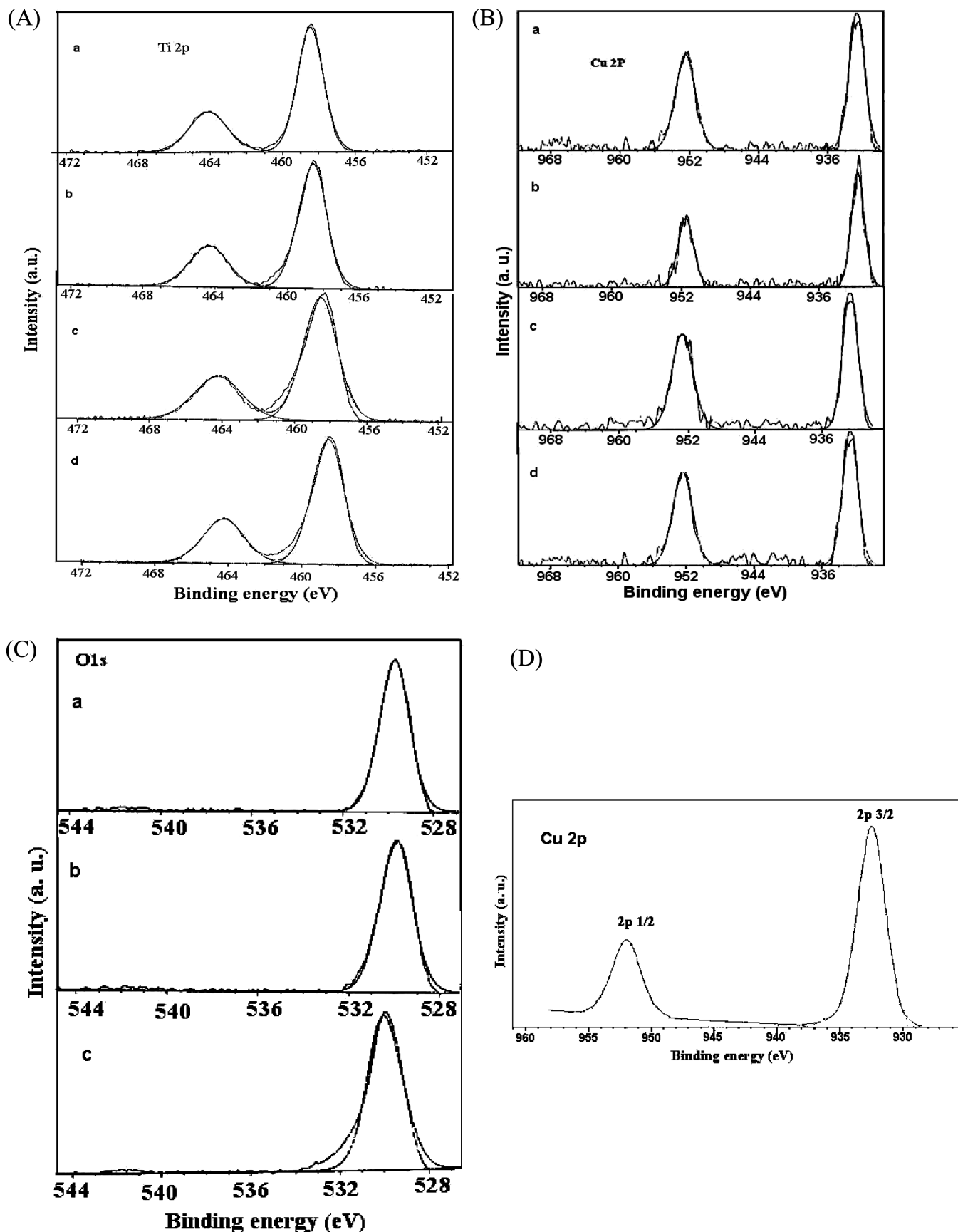


Figure 5. XPS of CT-2 catalysts. (A) Ti 2p at Cu wt % (a) 0.5, (b) 1, (c) 2, (d) 5. (B) Cu 2p at Cu wt % (a) 0.5, (b) 1, (c) 2, (d) 5. (C) O 1s at Cu wt % (a) 0.5, (b) 1, (c) 2. (D) Cu 2p spectra of 0.5 wt % CT-2 used catalysts.

are shown in parts A–C of Figure 5. The characteristic peaks of Ti 2p_{3/2} and 2p_{1/2} in TiO₂ (P-25) appear at binding energy values of 458.2 and 464.2 eV, respectively.²⁶ In CT-2 catalysts

the Ti 2p_{3/2} and 2p_{1/2} binding energy values are slightly shifted to higher binding energy regions and appear at 458.6 and 464.2 eV (Figure 5A). Cu 2p_{3/2} characteristic peaks for Cu⁰, Cu₂O,

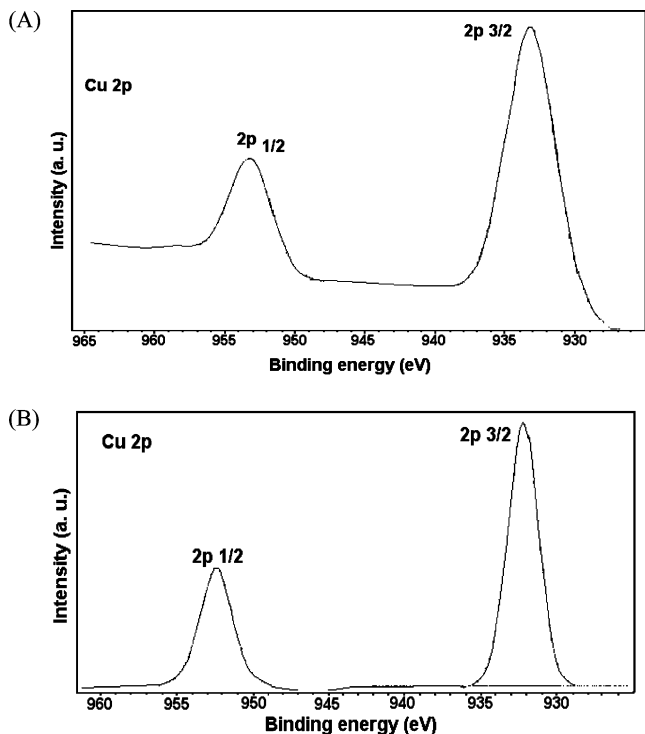


Figure 6. Cu 2p XP spectra of 0.5 wt % CT-1 catalysts (A) calcined and (B) used.

and CuO appear at 932, 932.7, and 933.6 eV.²⁶ The Cu 2p_{3/2} and Cu 2p_{1/2} binding energy values of CT-2 catalysts appeared at 932.4 and 952.0 eV, confirming the presence of Cu¹⁺ in CT-2 catalysts (Figure 5B). These results are in confirmation with earlier reports, where lower oxidation state of Cu is observed at higher calcination temperatures.¹⁶ O1s spectra of TiO₂ show the characteristic peaks of Ti–O linkages at a binding energy value of 529.9 eV. In CT-2 catalysts the binding energy values for O1s (Figure 5C) are shifted slightly toward higher binding energy values and appear at 530.6 eV. Figure 5D shows the Cu 2p XPS spectra of 0.5 wt % CT-2 used catalyst. On this catalyst the binding energy values appeared at 932.4 and 952.2 eV for Cu 2p_{3/2} and Cu 2p_{1/2}, respectively, indicating that the oxidation state of Cu is the same (+1) even after using the catalyst for several hours under solar irradiation.

Cu 2p XPS spectrum of 0.5 wt % CT-1 catalyst is shown in Figure 6A. In CT-1 catalyst, the binding energy values appeared at 933.2 and 953.1 eV for Cu 2p_{3/2} and Cu 2p_{1/2} indicating that copper is in +2 oxidation state.^{26,27} In CT-1 used, the BE values appeared at 932.8 and 952.2 eV (Figure 6B) indicating that CuO is converted into Cu₂O under solar irradiation.

3.6. Photocatalytic Activity. Photocatalytic hydrogen evolution studies are conducted over TiO₂ and Cu-loaded TiO₂ catalysts from pure water as well as glycerol:water mixtures under solar irradiation. Figure 7A shows the effect of Cu loading on photocatalytic hydrogen evolution from pure water on CT-1 and CT-2 catalysts. Hydrogen production is not observed on

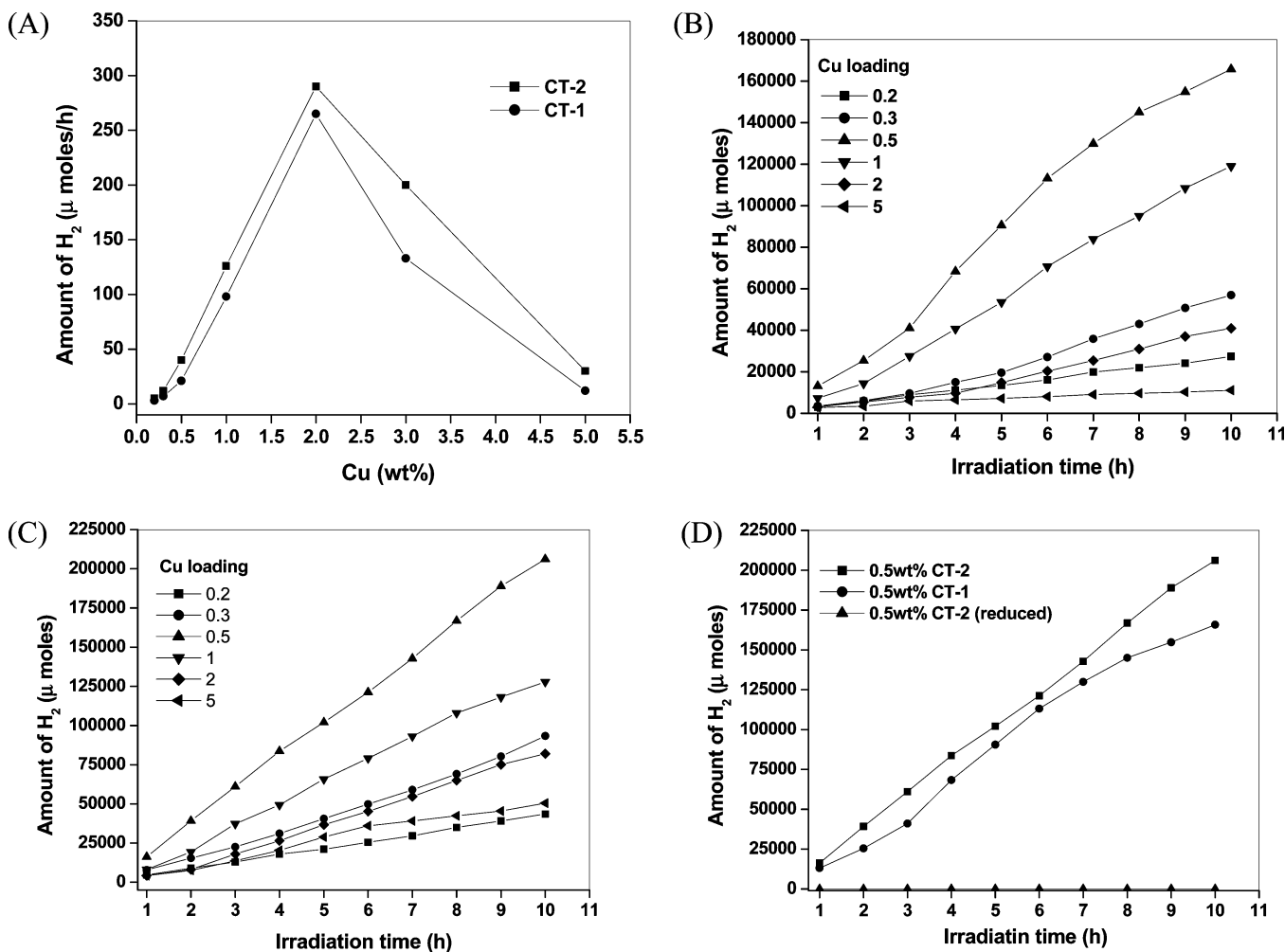


Figure 7. Cu loading vs hydrogen production activity over (A) CT-1 and CT-2 from pure water, (B) CT-1, (C) CT-2, and (D) 0.5 wt % CT-1, CT-2, and CT-2 reduced catalyst from glycerol:water mixtures under solar irradiation.

TABLE 2: H₂, O₂, and CO₂ Production over CT-1 and CT-2 Catalysts under Solar Irradiation

catalyst	H ₂ production (μmol/h)		O ₂ production (μmol/h)		CO ₂ production (μmol/h)	
	water	glycerol + water	water	glycerol + water	water	glycerol + water
TiO ₂	nil	600	nil	nil	nil	220
0.2 CT-1	3	2800	2	nil	nil	—
0.2 CT-2	5	4200	8	nil	nil	—
0.3 CT-1	7	5600	5	nil	nil	—
0.3 CT-2	12	9300	10	nil	nil	—
0.5 CT-1	21	16500	17	nil	nil	6050
0.5 CT-2	40	20060	30	nil	nil	7500
1 CT-1	98	11900	51	nil	nil	—
1 CT-2	126	12700	85	nil	nil	—
2 CT-1	265	4100	189	nil	nil	—
2 CT-2	290	8200	155	nil	nil	—
5 CT-1	12	1100	8	nil	nil	—
5 CT-2	30	4900	21	nil	nil	—

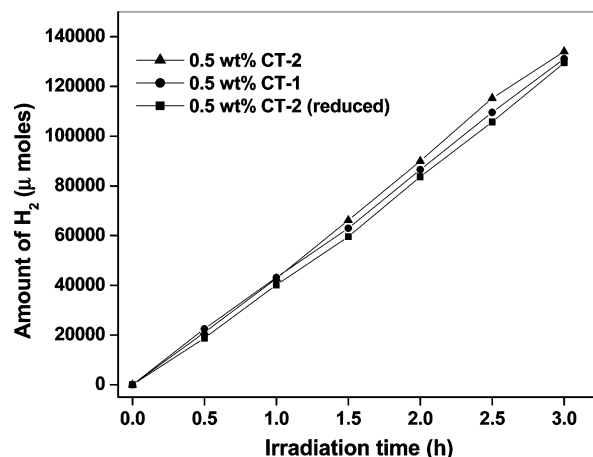
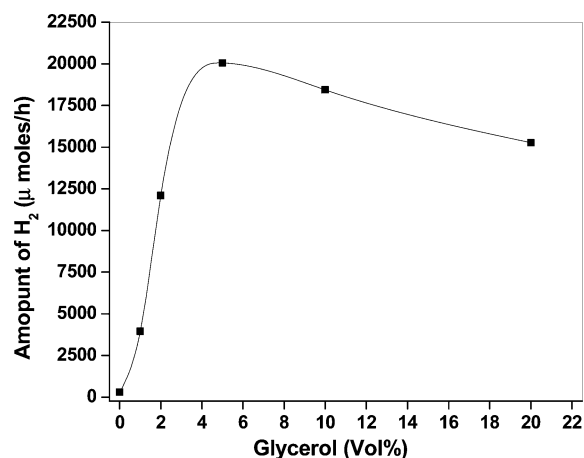
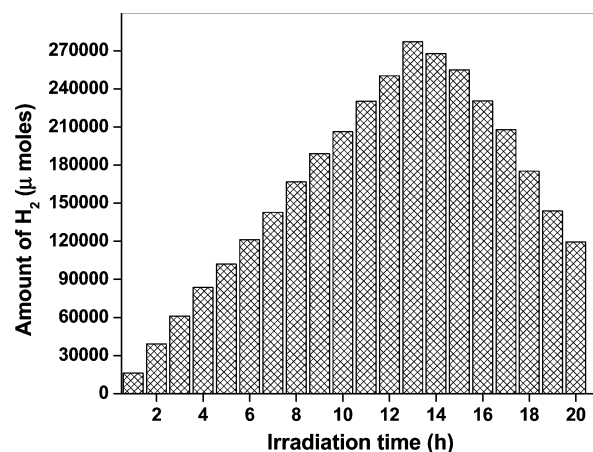
bare TiO₂ catalyst, whereas hydrogen and oxygen production is observed on copper-loaded TiO₂ catalysts as shown in Table 2.

TiO₂ and Cu-loaded TiO₂ catalysts are also evaluated for hydrogen production from glycerol:water mixtures under solar irradiation. Figure 7B shows the hydrogen production as a function of irradiation time over different CT-1 catalysts. Hydrogen production increased with increasing copper loading up to 0.5 wt % (16,485 μmol/h), and above this loading the activity is seen decreasing. Figure 7C shows the hydrogen production over different CT-2 catalysts from glycerol:water mixtures. Over these catalysts also the optimum amount of copper loading is found to be same. The hydrogen production over 0.5 wt % CT-2 catalyst is about 20,060 μmol/h. Of all the CT-1 and CT-2 catalysts studied, maximum hydrogen production activity is observed on 0.5 wt % CT-2 catalyst. When the reaction on CT-1 catalyst is compared with CT-2 catalyst, it is observed that the initial activity on CT-1 catalyst is only 50% that of CT-2 and after a period of 2–4 h, the activity is seen increasing to 80% of CT-2 catalysts. This may be seen as due to the reduction of Cu²⁺ on CT-1 to Cu⁺ during the course of reaction, which is confirmed by the XPS study of CT-1 used catalyst (Figure 6B). Thus hydrogen production activity can be studied on both CT-1 and CT-2 catalysts. As the CT-2 catalyst is showing high activity this system is further investigated to confirm Cu species in the +1 oxidation state is active for hydrogen production under solar irradiation. Thus thermally reduced CT-2 catalyst is also studied, and the results show that Cu in reduced state is not active for hydrogen production activity under solar irradiation. A comparative hydrogen production activity of 0.5 wt % CT-1, CT-2, and CT-2-reduced catalysts is shown in Figure 7D.

Activity studies are also conducted over 0.5 wt % CT-1, CT-2, and CT-2-reduced catalysts in glycerol:water mixtures under UV irradiation and shown in Figure 8.

About a 2–3-fold increase in the activity is observed under these conditions on CT-1 as well as CT-2 catalysts. Reduced catalyst is also showing almost equal activity as that of the calcined catalysts under UV irradiation. Under UV irradiation TiO₂ is the light-harvesting source and the loaded metal whether in the form of metal or metal oxide minimizes the electron–hole recombination and thus enhances the photocatalytic activity. These observations are in agreement with our earlier studies.²⁵

The effect of glycerol concentration on hydrogen production activity over 0.5 wt % CT-2 catalyst was also studied under

**Figure 8.** Cu oxidation state vs hydrogen production activity under UV irradiation.**Figure 9.** Glycerol concentration vs hydrogen production activity under solar irradiation.**Figure 10.** H₂ production activity over 0.5 wt % CT-2 catalyst under solar irradiation.

solar irradiation and is shown in Figure 9. With increasing glycerol concentration the hydrogen production activity increased and reached optimum at 5 vol %, and with further increase in glycerol concentration, the hydrogen production activity is seen decreasing. Earlier researchers found that after reaching the optimum concentration further increase in alcohol concentration decreases the activity, and they illustrated that this behavior results from the saturation of active sites.⁷

As 0.5 wt % CT-2 catalyst is showing optimum hydrogen production it is further subjected to time on stream activity.



The figure illustrates the photocatalytic mechanism for the conversion of glycerol to H₂ and CO₂ using a CuO/TiO₂ photocatalyst.

Photocatalytic Cycle:

$$\text{CuO/TiO}_2 \xrightarrow{\text{UV}} \text{Cu}_2\text{O/TiO}_2 \xrightarrow{\text{solar}} \text{CuO/TiO}_2$$

Photolysis of Water:

$$\text{TiO}_2 \xrightarrow{h\nu} \text{e}^- + \text{h}^+$$

$$\text{H}^+ + \text{e}^- \longrightarrow \text{H}_2$$

Glycerol Conversion Mechanism:

The mechanism shows the stepwise conversion of glycerol (HO-CH₂-CH(OH)-CH₂-OH) to H₂ and CO₂ via various intermediates and radical species, involving the loss of water molecules and the addition of hydroxyl radicals (·OH) and protons (H⁺).

Key steps include:

- Initial attack of ·OH on glycerol to form a radical intermediate.
- Dehydration (-H₂O) and hydration (+H₂O) steps leading to various sugar intermediates (e.g., dihydroxyacetone, glyceraldehyde).
- Further radical reactions and dehydration steps leading to smaller molecules like glyceraldehyde and glycic acid.
- Final conversion of glyceraldehyde to glycic acid and then to H₂ and CO₂.

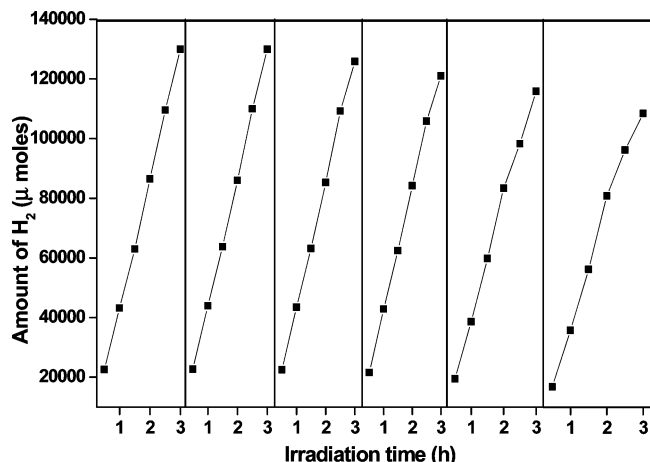


Figure 12. H_2 production activity in cycles over 0.5 wt % CT-2 catalyst under UV irradiation.

When the reaction is carried out continuously without evacuating the gases formed during the reaction, the activity is seen decreasing after 13 h (Figure 10), and this may be seen as due to the saturation of catalyst surface by the evolved gases suppressing the activity. When the activity tests were conducted by evacuating the evolved gases at regular intervals (5 h), a continuous and stable activity is observed under solar irradiation as shown in Figure 11. When this reaction was carried out under UV irradiation, after fourth cycle, the activity is seen decreasing (Figure 12). All the experiments were repeated 2–3 times, and the results are highly reproducible with $\pm 1\%$ variation.

3.7. Structure–Activity Correlation. The XPS results clearly illustrate that the oxidation state of Cu in the catalysts calcined at 350°C is +2, and it is +1 in samples calcined at 450°C . When the activity tests were conducted over these catalysts, CT-2 is showing higher and stable activity compared to CT-1 under solar irradiation. The initial activity over CT-1 catalysts is less, and after a period of 2–4 h, the activity increased steadily. This is seen as CuO becoming Cu_2O by consuming the electrons from initial irradiation. Once it is Cu_2O the activity is increased and resembles that of CT-2 catalysts. When these reactions are studied under UV irradiation CT-1 and CT-2 calcined and CT-2 reduced are showing almost same activity. Under UV conditions continuous activity is limited and decreases even after evacuating the evolved gases due to the possible dissolution of Cu ions in to the solution under the reaction conditions. From the characterization results and activity evaluations, a structure–activity correlation is observed, wherein the interacted copper ions with the surface of TiO_2 in the +1 oxidation state are playing an important role in harvesting the solar energy and responsible for continuous hydrogen production activity under solar irradiation as shown in Scheme 1.

4. Conclusions

By impregnating copper ions on TiO_2 surface, the absorption of TiO_2 is expanded into the visible region. EDAX confirms the presence of copper species on the surface of TiO_2 . TEM photographs show the fine dispersion of copper species on titania surface. XPS analysis confirms the interaction of copper ions with TiO_2 and in that Cu is in the +2 oxidation state when calcined at 350°C , and it is in the +1 oxidation state when calcined at 450°C . $\text{Cu}_2\text{O}/\text{TiO}_2$ is showing stable and continuous activity under solar irradiation, and no activity is observed on reduced catalyst which is seen due to the decreased band gap. From these results it may be concluded that interacted copper

ions in the +1 oxidation state with TiO_2 surface are responsible for continuous and stable hydrogen production activity under solar light irradiation. This study provides an efficient and low cost method for hydrogen production using solar energy.

Acknowledgment. K.L. thanks CSIR, New Delhi, for an SRF grant, and the authors thank MNRE, New Delhi, for funding this project.

References and Notes

- (1) Patsoura, A.; Kondarides, D. I.; Verykios, X. E. Photocatalytic degradation of organic pollutants with simultaneous production of hydrogen. *Catal. Today* **2007**, *124*, 94.
- (2) Wu, G.; Chen, T.; Su, W.; Zhou, G.; Zong, X.; Lei, Z.; Li, C. H_2 production with ultra-low CO selectivity via photocatalytic reforming of methanol on Au/TiO_2 catalyst. *Int. J. Hydrogen Energy* **2008**, *33*, 1243.
- (3) Ihara, T.; Miyoshi, M.; Iriyama, Y.; Matsumoto, O.; Sugihara, S. Visible-light-active titanium oxide photocatalyst realized by an oxygen-deficient structure and by nitrogen doping. *Appl. Catal. B* **2003**, *42*, 403.
- (4) Kato, H.; Kudo, A. Visible-Light-Response and Photocatalytic Activities of TiO_2 and SrTiO_3 Photocatalysts Co-doped with Antimony and Chromium. *J. Phys. Chem. B* **2002**, *106*, 5029.
- (5) Ohno, T.; Tanigawa, F.; Fujihara, K.; Izumi, S.; Matsumura, M. Photocatalytic oxidation of water by visible light using ruthenium-doped titanium dioxide powder. *J. Photochem. Photobiol. A* **1999**, *127*, 107.
- (6) Chiarello, G. C.; Forni, L.; Selli, E. Photocatalytic hydrogen production by liquid- and gas-phase reforming of CH_3OH over flame-made TiO_2 and Au/TiO_2 . *Catal. Today* **2009**, *144*, 69.
- (7) Strataki, N.; Bekiari, V.; Kondarides, D. I.; Liano, P. Hydrogen production by photocatalytic alcohol reforming employing highly efficient nanocrystalline titania films. *Appl. Catal. B* **2007**, *77*, 184.
- (8) Sreethawong, T.; Puangpet, T.; Chavadej, S.; Yoshikawa, S. Quantifying influence of operational parameters on photocatalytic H_2 evolution over Pt-loaded nanocrystalline mesoporous TiO_2 prepared by single-step sol-gel process with surfactant template. *J. Power Sources* **2007**, *165*, 861.
- (9) Blount, C. M.; Buchholz, J. A.; Falconer, J. L. Photocatalytic Decomposition of Aliphatic Alcohols, Acids, and Esters. *J. Catal.* **2001**, *197*, 303.
- (10) Li, Y.; Lu, G.; Li, S. Photocatalytic hydrogen generation and decomposition of oxalic acid over platinumized TiO_2 . *Appl. Catal. A* **2001**, *214*, 179.
- (11) Daskalaki, V. M.; Kondarides, D. I. Efficient production of hydrogen by photo-induced reforming of glycerol at ambient conditions. *Catal. Today* **2009**, *144*, 75.
- (12) Kondarides, D. I.; Daskalaki, V. M.; Patsoura, A.; Verykios, X. E. Hydrogen Production by Photo-Induced Reforming of Biomass Components and Derivatives at Ambient Conditions. *Catal. Lett.* **2008**, *122*, 26.
- (13) Bowker, M.; Davies, P. R.; Al-Mazroai, L. S. Photocatalytic Reforming of Glycerol over Gold and Palladium as an Alternative Fuel Source. *Catal. Lett.* **2009**, *128*, 253.
- (14) Luo, N.; Jiang, Z.; Shi, H.; Cao, F.; Xiao, T.; Edwards, P. P. Photocatalytic conversion of oxygenated hydrocarbons to hydrogen over heteroatom-doped TiO_2 catalysts. *Int. J. Hydrogen Energy* **2009**, *34*, 125.
- (15) Jin, Z.; Zhang, X.; Li, Y.; Li, S.; Lu, G. 5.1% Apparent quantum efficiency for stable hydrogen generation over eosin-sensitized CuO/TiO_2 photocatalyst under visible light irradiation. *Catal. Commun.* **2007**, *8*, 1267.
- (16) Wu, N. L.; Lee, M. S. Enhanced TiO_2 photocatalysis by Cu in hydrogen production from aqueous methanol solution. *Int. J. Hydrogen Energy* **2004**, *29*, 1601.
- (17) Choi, H.-J.; Kang, M. Hydrogen production from methanol/water decomposition in a liquid photosystem using the anatase structure of Cu loaded TiO_2 . *Int. J. Hydrogen Energy* **2007**, *32*, 3841.
- (18) Jeon, M. K.; Park, J.-W.; Kang, M. Hydrogen production from methanol/water decomposition in a liquid photosystem using the anatase and rutile forms of Cu-TiO_2 . *J. Ind. Eng. Chem.* **2007**, *13*, 84.
- (19) Yoong, L. S.; Chong, F. K.; Dutta, B. K. Development of copper-doped TiO_2 photocatalyst for hydrogen production under visible light. *Energy* **2009**, *34*, 1652.
- (20) Bandara, J.; Udawatta, C. P. K.; Rajapakse, C. S. K. Highly stable CuO incorporated TiO_2 catalyst for photocatalytic hydrogen production from H_2O . *Photochem. Photobiol. Sci.* **2005**, *4*, 857.
- (21) Xu, S.; Sun, D. D. Significant improvement of photocatalytic hydrogen generation rate over TiO_2 with deposited CuO . *Int. J. Hydrogen Energy* **2009**, *34*, 6096.
- (22) Xu, S.; Jiawei, N. G.; Zhang, X.; Bai, H.; Sun, D. D. Fabrication and comparison of highly efficient Cu incorporated TiO_2 photocatalyst for hydrogen generation from water. *Int. J. Hydrogen Energy* **2010**, *35*, 5254.

(23) Ratnamala, A.; Suresh, G.; Durga Kumari, V.; Subrahmanyam, M. Template synthesized nano-crystalline natrotantite: Preparation and photocatalytic activity for water decomposition. *Mater. Chem. Phys.* **2008**, *110*, 176.

(24) Krishna Reddy, J.; Suresh, G.; Hymavathi, Ch; Durga Kumari, V.; Subrahmanyam, M. Ce (III) species supported zeolites as novel photocatalysts for hydrogen production from water. *Catal. Today* **2009**, *141*, 89.

(25) Lalitha, K.; Krishna Reddy, J; Phanikrishna Sharma, M. V.; Durga Kumari, V.; Subrahmanyam, M. Continuous hydrogen production activity over finely dispersed Ag₂O/TiO₂ catalysts from methanol: water mixtures

under solar irradiation: A structure- activity correlation. *Int. J. Hydrogen Energy* **2010**, *35*, 3991.

(26) Moulder, J. F.; Stickle, W. F.; Sobol, P. E.; Bomben, K. D. *Handbook of X-ray Photoelectron Spectroscopy: A Reference book of standard spectra for identification and interpretation of xps data*; Perkin-Elmer Corporation, 1995.

(27) Coloma, F.; Marquez, F; Rochester, H. C.; Anderson, A. J. Determination of the nature and reactivity of copper sites in Cu-TiO₂ catalysts. *Phys. Chem. Chem. Phys.* **2000**, *2*, 5320.

JP107405U